DEPOSITION OF TITANIUM OXIDE FILMS BY REACTIVE HIGH POWER IMPULSE MAGNETRON SPUTTERING (HIPIMS): INFLUENCE OF THE PEAK CURRENT VALUE ON THE TRANSITION FROM METALLIC TO POISONED REGIMES

C. Nouvellon [a,], M. Michiels [a], J.P. Dauchot [a,d], C. Archambeau [b], F. Laffineur [b], E. Silberberg [b], S. Delvaux [c], R. Cloots [c], S. Konstantinidis [d], R. Snyders [a,d]

[a] *Materia Nova, Parc Initialis, av. Copernic. B-7000 Mons, Belgium*

[b] *ArcelorMittal Liège Research, B57 bd. de Colonster. B-4000, Liège, Belgium*

[c] *Laboratoire de Chimie Inorganique Structurale, University of Liège, Allée de la Chimie, 3, Bât 6A, B-4000, Belgium*

[d] *Chimie des Interactions Plasma Surface (ChIPS), CIRMAP, University of Mons, 20, place du Parc, B-7000, Mons, Belgium*

Keywords:
HiPIMS
HPPMS
Reactive magnetron sputtering
Transition between metallic and poisoned regimes Titanium oxide

Abstract

In this study, reactive High Power Impulse Magnetron Sputtering (HiPIMS) experiments were carried out to synthesize titanium oxide films, using a 45×15 cm² titanium target in Ar/O_2 gas mixtures. The deposition process was studied as a function of the peak current (i_{peak}) at constant voltage during the pulse (1 kV) and constant average power (P_{av}). As the oxygen flow was increased, i_{peak} was kept constant (160, 300 or 400A) by adjusting the pulse duration and the average power (2 or 4 kW) by adjusting the pulse repetition frequency. For all experimental conditions, an abrupt transition from metallic towards poisoned regimes was observed. The transition curves exhibit hysteresis. As i_{peak} is increased from 160 A to 450 A, for P_{av}=4 kW, the oxygen content (Ω) in the Ar/O_2 mixture needed to poison the target surface was reduced from Ω=11.5% to Ω=8.5%. These values are much smaller than those recorded for DC magnetron sputtering (DCMS) (Ω=42%) and pulsed DCMS (Ω=36%) experiments carried out at the same power. These results are explained by the enhancement of the ionization and dissociation rates of oxygen molecules with the increase of i_{peak}.

X-ray fluorescence data show that the higher is i_{peak}, the lower is the deposition rate (R_D). Therefore, both the deposition and poisoning processes depend on i_{peak}. According to X-ray diffraction data, for DCMS, the films are amorphous and for HiPIMS the phase constitution evolves from an anatase/rutile mixture to pure rutile as i_{peak} is increased.

Abbreviations: i_{peak}, peak current value; i(t), time dependent target current; u(t), time dependent target voltage; τ, pulse duration; F, pulse repetition frequency; P_{av}, time averaged power: Pav ¼ fʃ0τiðtÞuðtÞdt; V_D, time averaged voltage in the pulse;

1. Introduction

High Power Impulse Magnetron Sputtering (HiPIMS also known as HPPMS for High Power Pulsed Magnetron Sputtering) [[1] and references therein] is an IPVD (Ionized Physical Vapour Deposition) technique [2]. The power is applied to the target in the form of short pulses of high voltage and high current. During the pulse, the power density per unit area of the target can rise up to several $kW.cm^{-2}$ but, by adjusting pulse width and frequency, the average power density is maintained at values used in conventional DC magnetron sputtering (a few $W.cm^{-2}$). This way, the density of the magnetron plasma is strongly raised. This has two main consequences on the plasma chemistry: (1) the ionization rate of the,materials sputtered from the target is increased [1] and (2) in reactive mode, the reactive gas molecules are ionized and dissociated [3]. This behavior was observed for nitrogen [4].

The enhanced ionization rate [5–8] results in an intense ion bombardment of the growing film which in turn contributes to the crystallization and densification of the coating. For example, high density oxide thin films with increased refractive index can be obtained [9–11]. In [9], for titanium oxide thin film deposition, the use of HiPIMS

enabled the growth of pure rutile phase films while pulsed DCMS experiments performed in the same working conditions lead to the growth of the anatase phase.

Titanium oxide films are widely studied because of their interesting properties which depend to a large extent on the film phase constitution (amorphous, anatase and rutile). The rutile phase, which is the high temperature equilibrium phase (above 900 °C) [12–14], has a high density and a high refractive index [15] and, as a consequence, is mainly used in optical applications. On the other hand, anatase, the low temperature equilibrium phase, is used for gas detection or as the active component in "self-cleaning" windows: organic pollutants are photocatalytically decomposed as UV radiation is absorbed by the film covering the window [16,17].

In the case of the work reported in [9] and related to the synthesis of titanium oxide films by HiPIMS, no systematic investigation on the process parameters — plasma chemistry–film properties relationship was carried out. Alami et al. [18] showed, while reactively depositing CrN films, that the flux of ionized species increases as the peak target current is increased. In their working conditions, the film morphology varied dramatically as a function of the HiPIMS target peak current (while the average current was kept constant).

On the other hand, depositing ZrO_2 films by reactive HiPIMS, Sakarinos et al. [19] observed a smooth transition between the two modes and therefore no hysteresis. However, they observed that the transition appears at lower oxygen flows than in DCMS. The transition also moved to lower oxygen flow when, at constant average current, the current during the pulse was increased. In [20] an hysteresis free reactive HiPIMS process was reported for the synthesis of aluminum oxide films. To the contrary of what is reported in [19,20], Audronis et al. observed a hysteresis during the reactive HiPIMS of Ti in Ar/O_2 [21] and also for other material–gas systems [22,23].

From these reports, it is clear that it is still necessary to make efforts in order to understand the poisoning mechanism in reactive HiPIMS discharges. Therefore, the aim of the present study is to establish the relationship between the peak current (i_{peak}), the reactive HiPIMS discharge chemistry, and the characteristics of the titania films synthesized during reactive HiPIMS.

First, the oxygen content (Ω) needed to reach the so-called poisoned regime is determined at the same average power (P_{av}) for each sputtering regime namely DCMS, pulsed DCMS and HiPIMS. HiPIMS experiments are carried out for three values of the peak current (i_{peak}). Then, titanium oxide films are synthesized using reactive HiPIMS for several values (i) of i_{peak} and (ii) of the oxygen content in the discharge gas ($\%O_2$). Finally, the films are analyzed in order to correlate these experimental parameters with the deposition rate, the chemical composition, and the phase constitution of the films.

2. Experimental set-up

The coating chamber is a TSD 400-CD from HEF R&D (France). The pumping system consists of a combination of a primary mechanical pump with 40 $m^3.h^{-1}$ pumping speed (Leybold) and a turbomolecular pump with 1000 $l.s^{-1}$ pumping speed (Varian). The chamber has a volume of about 0.2 m^3 and the residual pressure is typically few 10^{-4} Pa. This turbomolecular pump is protected from coating deposition by baffles. When varying the oxygen flow, the argon flow is adjusted in order to keep constant the total flow to a value of 95 sccm (standard cubic centimeter per minute). The total pressure is kept to 0.5 Pa. A sectional view of the chamber with a general scheme of this one in inset is given in Fig. 1. A mapping of the cathode magnetic field is also given on the right side of the figure. The substrate holder facing the cathode at 9 cm from it, is a rotatable cylinder connected to the ground. Twelve 5×5 cm^2 stainless steel sheet substrates can be attached on it. The cathode is located vertically in one door of the chamber. The titanium target has an area of 45×15 cm^2 and is 8 mm thick. For the DC sputtering mode (DC or pulsed DC) an ENI RPG 100 generator is used. The pulsed DCMS plasma is produced with a 250 kHz repetition rate (t_{on}=2.384 µs and t_{off} (zero voltage)=1.616 µs). The recorded current and voltage waveforms are presented in Fig. 2. Both DC and Pulsed DC discharges are driven in the power regulation mode. The pulsing unit [24,25] used to generate the HiPIMS plasma is designed to deliver high peak power pulses. A maximum target voltage (V_D) of 1500 V or a maximum i_{peak} of 2300 A can be delivered. Hence more than one megawatt peak power can be reached. The pulse duration τ can be varied between 0.2 and 50 µs by steps of 0.2 µs and the pulse frequency f can vary from f=50 Hz to f=10 kHz by 50 Hz steps. For all i_{peak}, the voltage is at a quasi constant value of 1 kV during the pulse describing a square waveform (see Fig. 3c). The time-dependent target current i(t) is measured by a Hall effect probe (Tektronix TCP303) and the time-dependent target voltage, u(t), by a voltage probe (Tektronix P6015). Both parameters are measured at the magnetron power connection, as near as possible to the target. i(t) and u(t) waveforms are recorded on a digital oscilloscope (Tektronix TDS2024). The average power, P_{av}, is calculated with a 10 ns time resolution using Eq. (1):

$$P_{av} = f \int_0^{\tau} i(t)u(t)dt. \qquad (1)$$

In order to study the poisoning of the target, several experiments (called HiPIMS 1, 2 and 3) were performed using the process parameters summarized in Table 1. As $\%O_2$ varied from 0 to 50%, the pulse duration τ is adjusted, i.e. reduced if i_{peak} increases, in order to keep i_{peak} at a nearly constant value (the variations are maintained within a range of 15%) (Fig. 3a and b). Afterwards the frequency, f, is adapted in order to keep P_{av} constant. These variations of τ and f can be used to detect the metal-to-poisoned regime transition.
For HiPIMS 1 and 2, V_D is set to 1 kV. For HiPIMS 1, P_{av} =4 kW and i_{peak}=160 A, 300 A or 400 A. For HiPIMS 2, P_{av}=2 kW and i_{peak}=400 A. In HiPIMS 3, τ is kept constant to 13 µs. i_{peak} is set to 400 A by adjusting V_D and P_{av}=4 kW (by f adjustment). Conventional DC and pulsed DC experiments are carried out at P_{av}=4 kW in order to allow the comparison with the HiPIMS experiments. For the pulsed DC discharge, P_{av} is also calculated by using Eq. (1) (see Fig. 2). In DCMS and pulsed-DCMS, the transition is detected by the variation in target voltage as $\%O_2$ is increased. The film phase constitution is determined by grazing incidence X-Ray Diffraction (XRD) using a Bruker D8 Discover diffractometer. The amount of titanium deposited on the substrate per unit area expressed in mg/m² of titanium and the chemical composition of the films are extracted from X-Ray Fluorescence (XRF) data. XRF measurements are carried out using a Bruker S4-Pioneer spectrometer.

Fig. 1. Section view of the sputtering chamber and magnetic field mapping of the cathode. In inset: a global view of the chamber with the position of the section.

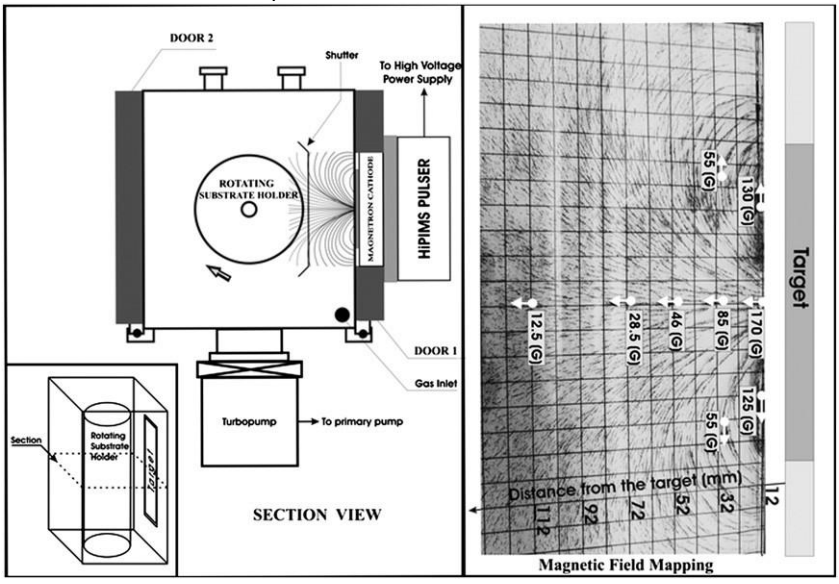

Fig. 2. Recorded voltage, current waveforms and resulting calculated power for the pulsed DCMS: f=250 kHz (t_{on} =2384 ns and t_{off} =1616 ns). a) Current. b) Voltage. c) Power.

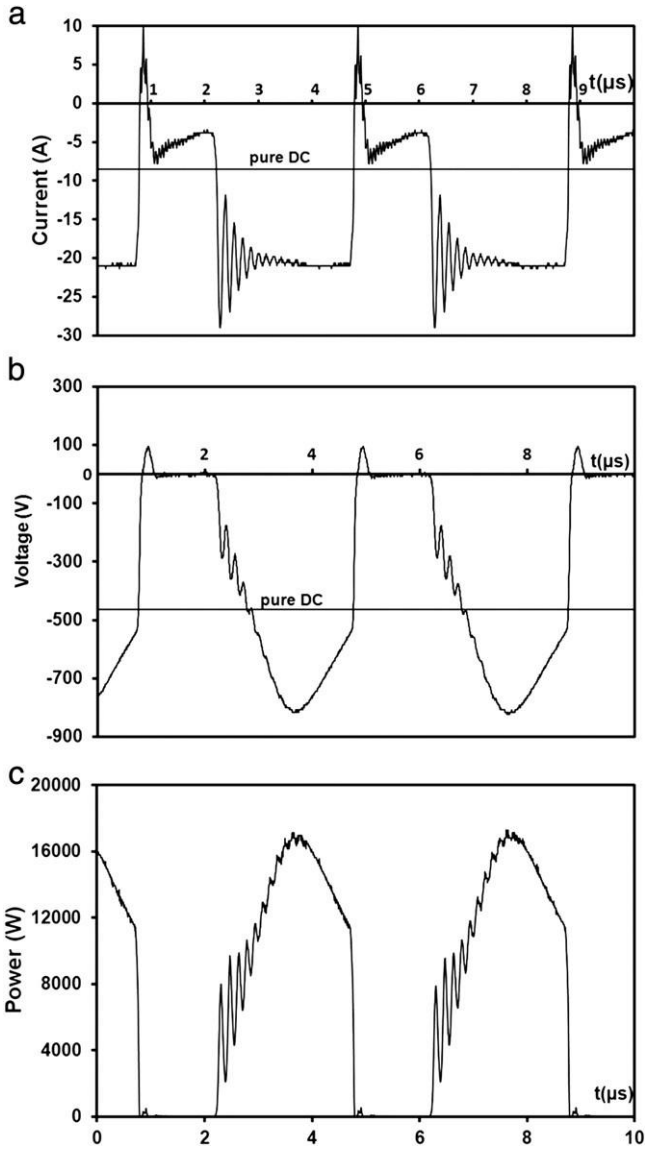

Fig. 3. At P_{av}=4 kW, before and after metallic to oxide transition: a) Current pulse profile for i_{peak}=160 A; b) Current pulse profile for i_{peak}=400 A; c) Voltage pulse profile for i_{peak}=400 A.

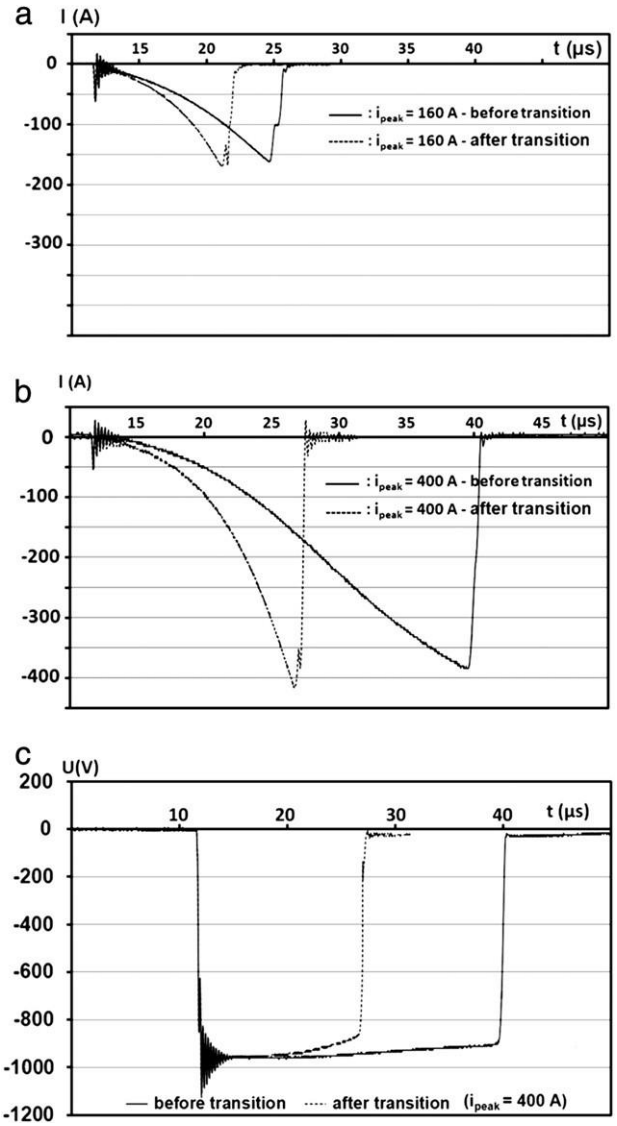

3. Results and discussion

3.1. Plasma chemistry and plasma–target surface interaction

For DC and pulsed DC discharges, when $\%O_2$ is increased, the transition between metallic and poisoned regimes is observed by an abrupt variation of the target voltage (the time averaged voltage for pulsed DC). In our working conditions, this transition appears for well-defined $\%O_2$ (Ω).

Table 1. Sputtering parameters for studying the transition.

	V_D (V)	Pav (kW)	ipeak (A)	f (Hz)	τ (µs)
DC		4			
HiPIMS 1	1000	4	160 300 400	Varies	Varies
HiPIMS 2	1000	2	400	Varies	Varies
HiPIMS 3	Varies	4	400	Varies	13

Ω=42% for DCMS and Ω=36% for pulsed DCMS. The higher value of Ω in DCMS as compared to pulsed DC can be explained by the fact that in order to reach the same average power as in DC, the voltage and the current in the pulse have to be increased (Fig. 2). Indeed, in pulsed DC, the time-averaged voltage and current (within a pulse), V_D and I_D are 550 V and 21 A, respectively (Fig. 2) and during the pulse, u(t) exhibits a maximum at 850 V while the current waveform peaks at 30 A. For comparison, during the DC experiments, the target voltage and current are 450 V and 9 A, respectively (see Fig. 2).

The same experiments are carried out using HiPIMS conditions (Table 1). Fig. 4a and b presents the evolution of τ and f as a function of $\%O_2$, respectively. One can remark that, whatever the value of i_{peak}, the transition occurs for lower Ω than the one recorded for the DCMS or pulsed DCMS: Ω ~9% for 300 A and 400 A and ~11% for 160 A. It is observed that the higher is i_{peak}, the lower is Ω. Therefore it can be concluded that increasing i_{peak} at a constant P_{av} implies that the amount of oxygen needed to poison the target is reduced. It is remarked that the value of Ω for the pulsed DCMS is intermediate between the ones observed in DCMS and HiPIMS. The way of delivering the power in pulsed DC (higher V_D and I_D) gives a plasma whose characteristics are nearer to the ones of the HiPIMS plasma.

In another experiment the average power is decreased from 4 kW to 2 kW but keeping i_{peak}=400 A, Ω decreases from Ω=9% to Ω=6.5%. Therefore it can be concluded that increasing the average power in HiPIMS leads to an increasing demand of O_2 for poisoning the target. This situation is similar to what is usually observed during conventional DC magnetron experiments.

Moreover in our experimental working conditions, a hysteresis is always observed and its width is reduced as i_{peak} is increased from 160 to 400 A at constant P_{av} of 4 kW. The hysteresis width decreases further as i_{peak} is increased up to 450 A by raising V_D but keeping τ constant to 13 μs and P_{av} to 4 kW (by f adjustment). Fig. 5 presents the evolution of Ω and the hysteresis width as a function of i_{peak} for the pulsed DCMS, and HiPIMS experiments. Ω for DCMS is also given in the graph. In this case, the current taken into account is the constant current measured when this technique is used.

To summarize, in our working conditions: (i) at a given P_{av}, the higher is $i_{peak,}$ the lower is Ω; (ii) at a given i_{peak}, the higher is P_{av} (increasing f), the larger is Ω; and (iii) the hysteresis width is reduced as i_{peak} is increased at a given P_{av}.

A higher i_{peak} can be associated with an increased plasma ionization rate as it was reported by Alami et al. [26] for Cr sputtering. It has also been showed for Ti sputtering in Ar that increasing the pulse duration for a given P_{av} leads to an increase of the ionization rate [5]. Therefore, it can be reasonably assumed that, even in a reactive atmosphere, the ionization rate of the metal atoms is dramatically increased by raising i_{peak}. The dissociation and ionization rate of the O_2 and sputtered compound clusters or molecules should be significantly increased as well as it has already been shown by Snyders et al. for ICP amplified discharges [27,28]. The main paths for dissociation and ionization of molecular oxygen by electron collision are, according to [29]:

$O_2 + e^- \rightarrow O^*_2 + e^- \rightarrow 2O + e^-$

$O_2 + e^- \rightarrow O^+_2 + 2e^-$

$O_2 + e^- \rightarrow O_2^{+**} + 2e^- \rightarrow O^+ + O + 2e^-$

$O_2 + e^- \rightarrow O^+ + 2e^-$

The cross section for these different processes, induced by electron impact, is a maximum for electrons having a kinetic energy of approx imately 100 eV ([3] and references therein). Although the pulses used in our experiments are shorter than those used in other HiPIMS related studies, fast electrons capable of inducing the above mentioned reactions should be generated. Poolcharuansin and Bradley [30] have found electrons of high energy at the beginning of the pulse (until about 4 μs after the start of the pulse) and Pajdarova et al. [31] observed hot electrons at the early stage of the HiPIMS discharge although the average electron energy was only a few eV.

The dissociation and ionization of the molecules during the short pulses of our HiPIMS process could explain the behavior of the current in the pulse after the transition (Fig. 3b). At the beginning of the pulse, the current rises quasi exponentially with time and the increase is faster after the transition than before. A similar behavior was reported in [3]. This behavior is at the opposite of what is observed in DCMS. It is known that, in the case of reactive Ar/O_2 DCMS operated at a constant current, the voltage rises at the transition in order to compensate the reduced secondary electron emission yield of the TiO_x compound formed on the target surface [27,28,32]. However, in every kind of sputtering discharge, at the transition, the oxygen partial pressure increases rapidly as

a consequence of the abrupt decrease of the deposition rate of the metallic titanium on the reactor walls canceling the well-known getter effect of the metal. Thanks to the high energy electrons present in the HiPIMS discharge, this rise of oxygen partial pressure could be accompanied by an increase in the population of oxygen ions (O_2^+ and O^+). These ions would contribute to the target ionic current. Moreover the ionization energies of O_2 and O are 12.6 eV and 13.6 eV, respectively [29]. As the work function of Ti and oxide covered Ti is between 4 and 4.5 eV, these two ions could improve the emission of secondary electrons through potential emission [29,33]. The so-generated secondary electrons could participate to the discharge current and, gaining energy in the cathodic sheath, are able to ionize and dissociate more oxygen thus inducing a cascade effect that would explain the exponential increase of the discharge current with respect to time. This mechanism could also explain that the current in the pulse rises more steeply in the poisoned regime as compared to what is observed in the metallic regime, where the self-sputtering regime makes the secondary electron emission yield to decrease according to a mechanism proposed in [33].

Regarding the poisoning mechanism and the reduced amount of oxygen, Ω, needed to reach the transition as i_{peak} is increased during HiPIMS at a given P_{av}, the first factors which could influence this value are the deposition flux of metallic Ti on the reactor walls and the reactivity of oxygen with the deposited titanium. Indeed, these two factors determine the getter effect of this deposit which controls the oxygen partial pressure in the reactor. It has been demonstrated [28] that the oxygen reactivity on titanium is very high and is not influenced by a denser plasma (ICP amplified discharge in this reference). However as the deposition rate of titanium is lowering when, in HiPIMS, i_{peak} is increased at a given P_{av}, the getter effect would reduce and Ω would lower. Another factor which could lead to a decrease of the getter effect in HiPIMS is the magnetic field geometry. Indeed, in HiPIMS, since the sputtered titanium is strongly ionized, if a strongly unbalanced magnetron is used [34], the ionized titanium deposition can be concentrated on a reduced area of the reactor surfaces (i.e. the substrate) so that the getter effect becomes less efficient. A magnetic mapping of our magnetron cathode is given in Fig. 1: it can be seen that this factor is not significant in our conditions.

It could also be argued that the sputtering wind and the gas rarefaction thereof [10], occurring predominantly for large pulse current conditions, would also concern O_2 and related species. Less O_2 would be available for target oxidation during the high peak current condition. However, i) if the dissociation and ionization rates of O_2 molecules are large and therefore the production of atomic oxygen enhanced and ii) if short pulses (as those used in the present study) are generated, the efficiency of the sputtering wind would decrease. As a consequence, the density of oxidizing species such as O and O^+ could rise up to a factor of 2 in the target vicinity (assuming an extreme case where every O_2 molecule is dissociated). For the highest i_{peak}, the O and O^+ concentrations can be increased in such a way that a lower oxygen flow is needed as these species can contribute to the target current and to target poisoning. Indeed, it has been demonstrated that the implantation of reactive O^+ ions is a key feature of the target poisoning mechanism [32,35]. Additionally, it should be kept in mind that the oxygen ionized species are trapped in the magnetic field near the target, participating to the Hall current, and at disposal for implantation in the target. The high voltage applied to the target (1 kV) during all the duration of the pulse makes this implantation more efficient.

Moreover, the erosion rate of the poisoned target (i.e. the target “cleaning”) would be physically reduced as Ti^+, O_2^+ and O^+ ions are contributing, to a large extent, to the flux of ions impacting the target during reactive HiPIMS while Ar^+, O_2^+ and O^+ ions are the dominant species during reactive DCMS. The sputtering yields of O and Ti (γ_O,γ_{Ti}) for 1 keV Ar^+, O^+ and Ti^+ ions impacting a TiO_2 solid target are calculated using SRIM (Stopping Range of Ions in Matter) [36]. They are reported in Table 3. Only a small discrepancy (a few %) is observed between the computed sputtering yields when a 1 keV Ar^+ impacting ion is replaced by a 1 keV Ti^+. It should be remarked that the sputtering of oxygen atoms by Ti^+ is operated with a good yield (1.64) and that the target is supplied by titanium since Ti^+ remains in the target. The cleaning is therefore more efficient. Based on these considerations, it can be concluded that the modification of the composition of the target ion flux while working in HiPIMS and DCMS conditions cannot explain the large decrease of Ω which is about a factor 4 when, for the same average power, HiPIMS with i_{peak}=400 A replaces DCMS.

Finally, the change in the target erosion area (i.e. the race track) can also be invoked to explain the observed lowering of Ω for higher i_{peak}. A variation in the width of the spatial distribution of the target current density over the racetrack during the pulse was reported in [37]: the maximum width is observed shortly after the current peak. In this paper, the authors measured a broader erosion profile in HiPIMS than in DC sputtering. For the largest peak current (i.e. i_{peak}=400 A), the plasma confinement on the target could be weakened and, in turn, the

power density in the erosion zone would decrease as the plasma spreads over a larger area, leading to a lowering of the erosion rate of the oxide layer covering the target and in turn to a lowering of Ω.
Finally, the evolution of the hysteresis width with i_{peak} (as reported in Fig. 5) could be explained, to some extent, by the increase of the dissociation rate of the sputtered compound clusters (such as TiO, TiO_2…) in the HiPIMS plasma. Berg and Nyberg modeled the influence of this factor for a reactive DC sputtering discharge [38].

Fig. 4. As the oxygen content in the gas mixture supply is varied: a) Transition observed by the pulse duration change made to keep constant i_{peak}. b) Transition observed by the frequency change made to keep constant P_{av}.

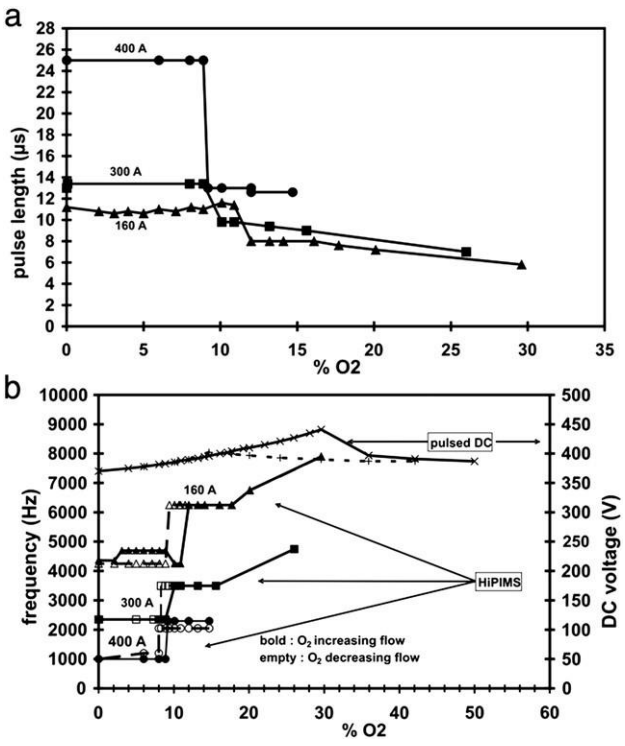

Fig. 5. Oxygen content in the gas mixture at the transition (Ω) and hysteresis width as a function of i_{peak} for pulsed DCMS and HiPIMS. Ω for DCMS is also plotted for the value of the DC current.

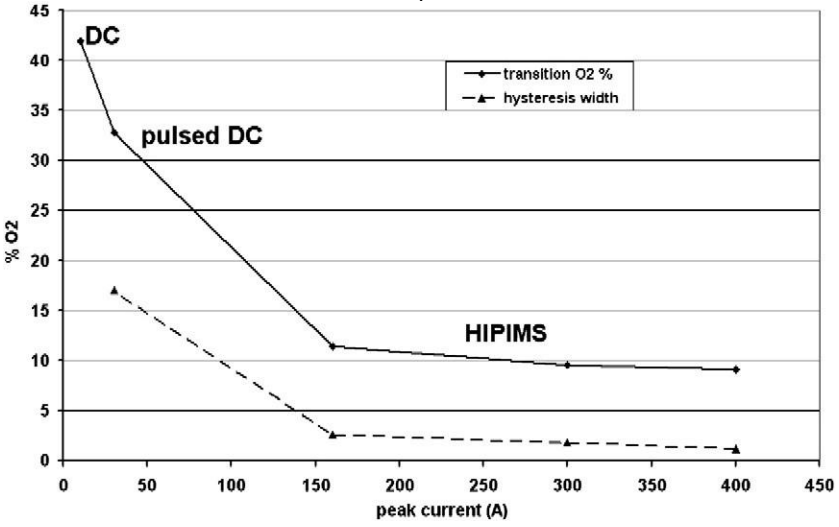

Table 2 Sputtering parameters for TiO_x deposition. Calculated thickness and stoichiometry of the deposited films.

Deposition technique	P_{av} (kW)	i_{peak} (A)	Deposition time (h)	$\%O_2$ in the gas mixture supply	τ (μs)	Film thickness (nm)	Deposited films stoichiometry TiO_x (x=)
Pulsed DC	4		1 h30 2 h[a]	42		205 (273)[a]	1.99
HiPIMS	4	160	2	12.5		274	2.07
				15		220	2.07
				30		136	2.07
	4	400	2	11.5		141	2.07
	4	400	2	14.5		100	2.07
	2	400	4	8		101	2.07
				12		88	2.15
	4	420	2	10	13	131	2.07
	4	450	2	15	13	95	2.07
	4	480	2	30	13	54	2.15

[a]Thickness extrapolated to h2

Table 3 Sputtering yield of Ti and O by Ar^+, O^+ and Ti^+ from a TiO_2 target.

$\gamma_{Ti}^{Ar} = 0.42$	$\gamma_{O}^{Ar} = 1.74$
$\gamma_{Ti}^{O_+} = 0.44$	$\gamma_{O}^{O^+} = 1.62$
$\gamma_{Ti}^{Ti_+} = 0.42$	$\gamma_{O}^{Ti_+} = 1.64$

3. 2. Thin films' growth and characterization

As the boundary of the poisoned regime has been determined for each experimental condition, TiOx films are deposited in the oxide mode for different %O2 (right after the transition or higher). The operating conditions are given in Table 2. The deposition time is 2 h for P_{av}=4 kW and 4 h in case of P_{av} =2 kW. In this way the same power×time product is obtained and a similar amount of energy should be provided to the growing films. Although the deposition time is 1.5 h for the DCMS mode of operation, the deposition rate for a 2 h deposition process was extrapolated in order to allow the comparison with other experiments.

The deposition rate (R_D) and the chemical composition of the films are both estimated by X-ray fluorescence measurements. All the films are close to the TiO_2 stoichiometry with a trend to a light oxygen over stoichiometry which does not depend on the working conditions. The average R_D is calculated assuming a mean TiO_2 film density (between 3.65 for the amorphous phase and 4.2 for the rutile phase). The film thicknesses determined in this way are reported in Table 2. R_D versus $\%O_2$, in various HiPIMS conditions, is reported in Fig. 6. A data point related to the DCMS grown film is plotted as a reference (Fig. 6, up right). Whatever the conditions, R_D decreases as $\%O_2$ increases. Moreover, at constant P_{av}, R_D is higher for a lower i_{peak} value: R_D at P_{av} =4 kW and i_{peak}=160 A is about twice the value of the one at P_{av} =4 kW and i_{peak}=400 A. For the low i_{peak} condition (P_{av} =4 kW; i_{peak}=160 A), R_D just after the transition ($\%O_2$=11%) is even the same as for DCMS in the poisoned mode (P=4 kW; $\%O_2$=42%).

For the same P_{av} (4 kW), R_D decreases when i_{peak} is increased. This is likely due to the increased ionization rate of the plasma gas and especially of the sputtered material. For these high i_{peak} and peak power values, self-sputtering can occur, hence reducing the sputtering rate and in turn R_D as metal ions are attracted back on the target instead of condensing on the substrate surface. This phenomenon is well described for experiments carried out in the metallic mode. The target sputtering is induced not only by Ar^+ ions but also by Ti^+ ions [1]. High ionization combined to Ar gas rarefaction induces selfsputtering and loss of deposition rate [25]. Gas rarefaction would also

occur in reactive HiPIMS [10]. For high i_{peak} conditions, titanium oxide and oxygen ions could also participate to sputtering, with probable lower efficiency, explaining the loss in R_D. The low R_D in HiPIMS could be also explained by the observations of Mishra et al. [39] in non reactive HiPIMS of a titanium target in Ar. During the voltage pulse, negative plasma potential values were measured: "In the initial phase of the pulse, t=6–8 μs, large potentials (−210 V) are generated across the plasma bulk particularly inside the magnetic trap". "The spatial structure of the plasma potential provides a large potential barrier for sputtered ionized species so impeding their transport and deposition at the substrate". It should be pointed out that, if the situation is the same in reactive (Ar/O_2) HiPIMS, this potential barrier across the plasma impedes the positive ions to reach the substrate. However negative ions like oxygen (O_2^- and O^-) can be accelerated and bring energy to the growing film on the grounded substrate. Sarakinos et al. [40] have detected such negative ions by mass spectrometry during reactive HiPIMS and DCMS discharges.

The phase constitution of the films deposited in HiPIMS is reported in Fig. 7 with respect to $\%O_2$ and i_{peak}. Although the coatings were synthesized with the same power×duration product, the film thickness varies as a function of the working conditions (see Table 2). The XRD intensity being thickness dependent, only qualitative information related to the film phase constitution must be considered. In the present study, only two peaks are detected through the different diffractograms. They correspond to the crystallographic (100) reflection of anatase or to the (110) reflection of rutile.

In DC mode (205 nm thick film), no diffraction peak is detected. For the HiPIMS deposited films, at low i_{peak} (160 A), slightly after the transition ($\%O_2$=12.5%), no diffraction peak is observed. However, the (110) rutile reflection appears when $\%O_2$ is slightly increased to 15%. As $\%O_2$ is further increased (30%) both rutile and anatase phases are detected. Although the thickness is low (136 nm), the diffraction peaks are still well defined.

For the highest i_{peak} (400 A), rutile is already observed for $\%O_2$ =11.5% at P_{av} =4 kW and for $\%O_2$ =8% at P_{av} =2 kW. For $\%O_2$ =15 % at P_{av} =4 kW and $\%O_2$=12% at P_{av} =2 kW, the rutile reflection is still observed but, as the films obtained in these conditions are thinner, its intensity decreases. For the experiments driven at P_{av}=4 kW with constant pulse duration of 13 μs, the same trend is observed although larger peak current values were used in this case (up to 480 A).

In summary, for low i_{peak}, using a large $\%O_2$ promotes a mixture of anatase and rutile phases. For high i_{peak}, rutile is always obtained whatever $\%O_2$. The same kind of result has been obtained recently [41,42].

Low R_D conditions and intense ionic bombardment are often invoked as the conditions enabling the growth of rutile TiO_2 [9,43]. Using high i_{peak} (400 A) these conditions are fulfilled. On the other hand, it is suggested from previous DC sputtering experiments [44] that in reactive mode, the flux of negative oxygen ions (e.g. O^-) would influence the film structure. For reactive HiPIMS of Ti, Stranak et al. [45] have observed that the phase constitution of TiO_2 was influenced by the pressure: rutile was obtained at low pressure and anatase at high pressure. This was explained by the difference in the energy of the particles striking the substrate. Alami et al. [43] have also shown a change in the phase constitution as a function of the working pressure.

In our experiments, the total pressure is maintained constant (0.5 Pa) but the flux of ions (positively and negatively charged) and electrons on the substrate is probably different as i_{peak} varies between 160 and 400 A. When increasing i_{peak}, the ionization rate increase likely leads to an intensified ion bombardment.

Fig. 6. R_D versus $\%O_2$, in various HIPIMS conditions, at the same power×time product.

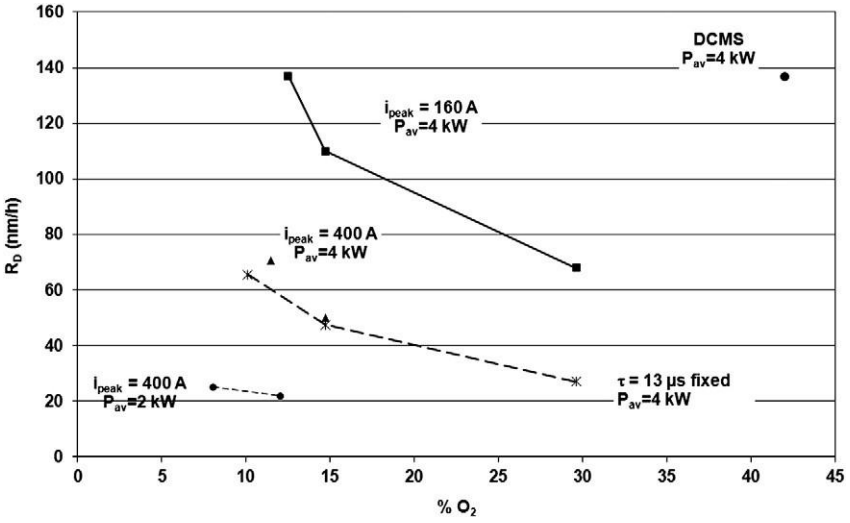

Fig. 7. Crystallographic characteristics of the films obtained for various HIPIMS conditions and oxygen content in the gas mixture supply (a: amorphous; A: anatase (100); R: rutile(110), (R): small rutile peak).

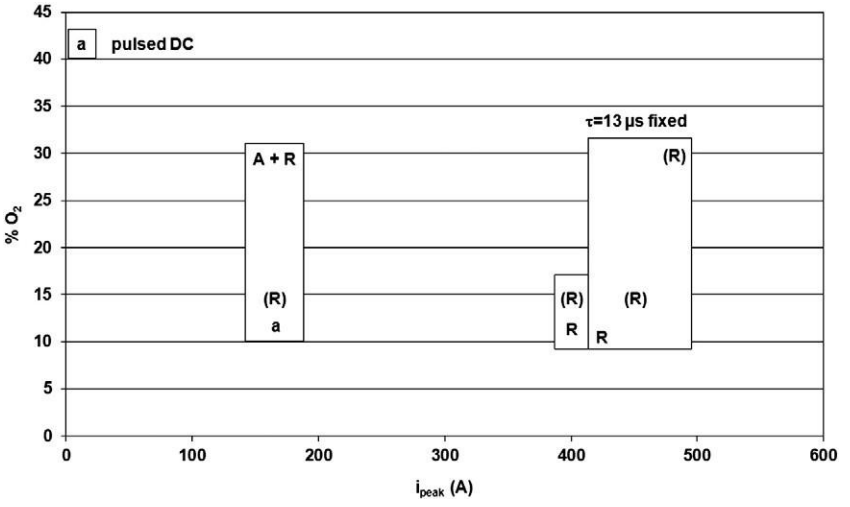

4. Conclusions

The synthesis of titanium oxide films by HiPIMS and DCMS in a reactive Ar/O_2 atmosphere has been studied for various values of peak current, i_{peak}, and for different amount of oxygen introduced in the gas mixture ($\%O_2$), at constant average power, P_{av} (either 4 kW or 2 kW). DCMS experiments were carried out at the same power values for comparison.

A transition with hysteresis between metallic and oxide modes is always observed either in HiPIMS or in DCMS. In HiPIMS, the critical oxygen content needed to reach this transition (Ω) rises as P_{av} is increased. At the opposite, at a given P_{av}, the higher is i_{peak}, the lower is Ω. The hysteresis is narrower at higher i_{peak}. It is also observed that the current in the pulse rises faster after the transition. These results could be explained by an increased ionization and dissociation rate of both O_2 and the sputtered clusters and molecules. These dissociation and ionization reactions would be enabled by high energy electrons populating the plasma induced by the short pulses used in the present work.

Films deposited on stainless steel foils, in the oxide regime, are stoichiometric. Those deposited in DCMS are always XRD amorphous. In HiPIMS, the film crystalline properties depend on i_{peak} and $\%O_2$. At low I_{peak} (160 A), the film crystallinity varies with $\%O_2$: being XRD amorphous at low $\%O_2$ and presenting a mixture of anatase and rutile phases as $\%O_2$ is increased. As i_{peak} is increased (400 A), the rutile phase appears whatever the $\%O_2$ value.

These evolutions have been attributed to different positive and negative ion fluxes towards the substrates when playing with i_{peak}.

Acknowledgment
The authors thank the "Ministère de La Région Wallonne" for the financial support in the frame of the "MIRAGE" project. S. Konstantinidis is a research associate of the National Funds for Scientific Research (FNRS Belgium). S. Konstantinidis and R. Snyders thank the Interuniversity Attraction Poles Program of the Belgian Science Policy (Project "PSI: Fundamentals of Plasma Surface Interactions") for financial support.

References

[1] K. Sarakinos, J. Alami, S. Konstantinidis, Surf. Coat. Technol. 204 (2010) 1661.
[2] U. Helmersson, M. Lattemann, J. Bohlmark, A.P. Ehiasarian, J.T. Gudmundsson, Thin Solid Films 513 (2006) 1.
[3] D. Benzeggouta, M.C. Hugon, J. Bretagne, M. Ganciu, Plasma Sources Sci. Technol. 18 (2009) I: N° 045025 & II: N° 045026.
[4] A.P. Ehiasarian, Y.A. Gonzalvo, T.D. Whitmore, Plasma Processes Polym. 4 (2007) S309.
[5] S. Konstantinidis, J.P. Dauchot, M. Ganciu, A. Ricard, M. Hecq, J. Appl. Phys. 99 (2006) 013307.
[6] K. Sarakinos, J. Alami, C. Klever, M. Wuttig, Rev. Adv. Mater. Sci. 15 (2007) 44.
[7] S. Konstantinidis, J.P. Dauchot, M. Ganciu, M. Hecq, Appl. Phys. Lett. 88 (2006) 021501.
[8] A.P. Ehiasarian, A. Vetushka, A. Hecimovic, S. Konstantinidis, J. Appl. Phys. 104 (2008) 83305.
[9] S. Konstantinidis, J.P. Dauchot, M. Hecq, Thin Solid Films 515 (2006) 1182.
[10] K. Sarakinos, J. Alami, M. Wuttig, J. Phys. D: Appl. Phys. 40 (2007) 2108.
[11] S. Konstantinidis, A. Hemberg, J.P. Dauchot, M. Hecq, J. Vac. Sci. Technol., B 25 (3) (2007) L19.
[12] M. Zribi, M. Kanzari, B. Rezig, Thin Solid Films 516 (2008) 1476.
[13] N. Martin, C. Rousselot, D. Rondot, F. Palmino, R. Mercier, Thin Solid Films 300 (1997) 113.
[14] Y.-Q. Hou, D.-M. Zhuang, G. Zhang, M. Zhao, M.-S. Wu, Appl. Surf. Sci. 218 (2003) 97. [15] G. Samsonov, The Oxide Handbook-IFI/Plenum New York, 1973, p. 333.
[16] A. Mills, J. Wang, M. Crow, G. Taglioni, L. Novella, J. Photochem. Photobiol., A 187 (2007) 370.
[17] T. Watanabe, A. Nakajima, R. Wang, M. Minabe, S. Koizumi, A. Fujishima, K. Hashimoto, Thin Solid Films 351 (1999) 260.
[18] J. Alami, K. Sarakinos, F. Uslu, M. Wuttig, J. Phys. D: Appl. Phys. 42 (2009) 015304. [19] K. Sarakinos, J. Alami, C. Klever, M. Wuttig, Surf. Coat. Technol. 202 (2008) 5033.
[20] E. Wallin, U. Helmersson, Thin Solid Films 516 (2008) 6398.
[21] M. Audronis, V. Bellido-Gonzalez, Thin Solid Films 518 (2010) 1962.
[22] M. Audronis, V. Bellido-Gonsalvez, B. Daniel, Surf. Coat. Technol. 204 (2010) 2159. [23] M. Audronis, V. Bellido-Gonsalvez, Surf. Coat. Technol. 205 (2011) 3613.
[24] M. Ganciu, M. Hecq, S. Konstantinidis, J. P. Dauchot, M. Touzeau, L. de Poucques, J. Bretagne, World patent No. WO 2005/090632.
[25] M. Ganciu, S. Konstantinidis, Y. Paint, J.P. Dauchot, A. Ricard, M. Hecq, L. de Poucques, P. Vasina, M. Mesko, J.-C. Imbert, J. Bretagne, M. Touzeau, J. Opt. Adv. Mater. 7 (2005) 2481.
[26] J. Alami, K. Sarakinos, G. Mark, M. Wuttig, Appl. Phys. Lett. 89 (2006) 154104.
[27] R. Snyders, R. Gouttebaron, J.P. Dauchot, M. Hecq, J. Anal. At. Spectrom. 18 (2003) 618.
[28] R. Snyders, J.P. Dauchot, M. Hecq, Plasma Processes Polym. 4 (2007) 113.
[29] M.A. Lieberman, A.J. Lichtenberg, Principles of Plasma Discharges and Materials Processing, John Wiley & Sons, New York, 1994.
[30] P. Poolcharuansin, J.W. Bradley, Plasma Sources Sci. Technol. 19 (2010) 025010.
[31] A.D. Pajdarova, J. Vlcek, P. Kudlacek, J. Lukas, Plasma Sources Sci. Technol. 18 (2009) 025008.
[32] D. Depla, S. Heirwegh, S. Mahieu, J. Haemers, R. De Gryse, J. Appl. Phys. 101 (1) (2007) N° 013301.
[33] A. Anders, Surf. Coat. Technol. 205 (2011) S1.
[34] J. Bohlmark, M. Östbye, M. Lattermann, H. Ljungcrantz, T. Rosll, U. Helmersson, Thin Solid Films 515 (2006) 1928.
[35] D. Depla, S. Mahieu, R. Degryse, Thin Solid Films 517 (2009) 2825.
[36] www.SRIM.org.

[37] G. Clarke, A. Mishra, P.J. Kelly, J.W. Bradley, Plasma Processes Polym. 6 (2009) S548.
[38] S. Berg, T. Nyberg, Thin Solid Films 476 (2005) 215.
[39] A. Mishra, P.J. Kelly, J.W. Bradley, Plasma Sources Sci. Technol. 19 (2010) 045014.
[40] K. Sarakinos, D. Music, S. Mraz, M. To Baben, K. Jiang, F. Nahif, A. Braun, C. Zilkens, S. Konstantinidis, F. Renaux, D. Gossement, F. Munnik, J.M. Schneider, J. Appl. Phys. 108 (2010) 014904.
[41] M. Aiempanakit, U. Helmerson, A. Aijaz, P. Larson, R. Magnusson, J. Jensen, T. Kubart, Surf. Coat. Technol. 205 (2011) 4828.
[42] F.J. Jing, K. Yukimura, H. Kato, Y.F. Lei, T.X. You, Y.X. Leng, N. Huang, Surf. Coat. Technol. 206 (2011) 967.
[43] J. Alami, K. Sarakinos, F. Uslu, C. Klever, J. Dukwen, M. Wuttig, J. Phys. D: Appl. Phys. 42 (2009) 115204.
[44] J.M. Ngaruiya, O. Kappertz, S.H. Mohamed, M. Wuttig, Appl. Phys. Lett. 85 (5) (2004) 749.
[45] V. Stranak, M. Quaas, H. Wulff, Z. Hubicka, S. Wrehde, M. Tichy, R. Hippler, J. Phys. D: Appl. Phys. 41 (2008) 055202.